Downloaded from orbit.dtu.dk on: Apr 19, 2024

DTU Library

A method for identification and quantification of thermal lensing in powder bed fusion

Andersen, S. A. ; Valente, E. H.; Nadimpalli, V. K.; Hansen, H. N.; Pedersen, D. B.

Published in:
Proceedings of the 19th International Conference and Exhibition (EUSPEN 2019)

Publication date:
2019

Document Version
Publisher's PDF, also known as Version of record

Link back to DTU Orbit

Citation (APA):
Andersen, S. A., Valente, E. H., Nadimpalli, V. K., Hansen, H. N., & Pedersen, D. B. (2019). A method for identification and quantification of thermal lensing in powder bed fusion. In C. Nisbet, R. K. Leach, D. Billington, & D. Phillips (Eds.), *Proceedings of the 19th International Conference and Exhibition (EUSPEN 2019)* (pp. 230-233). The European Society for Precision Engineering and Nanotechnology.

General rights
Copyright and moral rights for the publications made accessible in the public portal are retained by the authors and/or other copyright owners and it is a condition of accessing publications that users recognise and abide by the legal requirements associated with these rights.

- Users may download and print one copy of any publication from the public portal for the purpose of private study or research.
- You may not further distribute the material or use it for any profit-making activity or commercial gain
- You may freely distribute the URL identifying the publication in the public portal

If you believe that this document breaches copyright please contact us providing details, and we will remove access to the work immediately and investigate your claim.

euspen's 19th International Conference & Exhibition, Bilbao, ES, June 2019
www.euspen.eu

A method for identification and quantification of thermal lensing in powder bed fusion

Sebastian Aagaard Andersen[1], Emilie Hørdum Valente[1], Venkata Karthik Nadimpalli[1], Hans Nørgaard Hansen[1] and David Bue Pedersen[1]

[1]*The Technical University of Denmark*
seaa@mek.dtu.dk

Abstract
With the increase in use of L-PBF for functional components, an increase in productivity demands higher laser power and continuous operation. However, both these factors can affect the optics involved. The principal components of a Laser Powder Bed Fusion system are the galvanometer mirrors and the focusing lens. In the present work a method for identification and quantification of thermal lensing is proposed. Laser powder bed fusion experiments of stainless steel 316L powder was carried out at varying scan speeds and scan strategies in order to study the effects, of long exposure times, on the quality of single layer scans. It was observed that the heating of silver-coated mirrors under continuous exposure led to a significant decrease in the beam quality as evidenced by weld track widening and loss in depth of melt pool penetration. Power measurements conducted at various locations along the beam path indicated that the mirrors were absorbing up to 42 % of the total power coming from the laser while also defocusing the beam. Thus demonstrating the importance of including identification and quantification of thermal influence and possible instability of the optical elements as cause for irregular weld tracks.

Laser Powder Bed Fusion, L-PBF, Additive Manufacturing, Thermal Lensing

1. Introduction

Investigation of laser powder bed fusion (L-PBF)[1] determines that the quality of the produced parts are influenced by a vast number of both process- and machine parameters. In this work the influence of thermal lensing[2][3], the thermal distortion of optical elements leading to a change in the laser beam, is investigated as a constituent affecting the weld line quality.

Based on the discovery that weld line widening in L-PBF can be caused by thermal lensing, this paper presents a method for identification and quantification of this cause and effect relation. As the majority of the commercially available L-PBF machine tools are highly proprietary, an open architecture platform has been developed, see figure 1.

At the heart of the L-PBF process is the consolidation zone, where the laser heats the feedstock above its melting temperature. Moving towards the laser source, see figure 1, an fθ scan lens is used to focus the beam, and keep the distortion of the beam spot geometry at a minimum. Moreover, the fθ scan lens ensures a constant relation between the incident angle and the moved distance in the image plane. Before entering the fθ scan lens, the laser beam travels within the scan head that is used to move the beam at any chosen trajectory. The scan head consist of two mirrors mounted on galvanometric motors that control the angle of the mirrors, and thus the location and scanning velocity of the laser beam within the image plane. The current experimental setup also includes alignment mirrors to ensure the laser beam is guided from the collimating delivery fiber to the scan head. If any of the intermediate optical components suffer distortions due to thermal lensing, the consolidation process will become unstable, and influence the quality of the processed parts.

To obtain uniform weld tracks it is essential to ensure stable process parameters. The simplified term for the area energy density, E_d (1)[4], is used as a comparative measure of some governing process parameters, indicating the amount of energy that dissipates into the feed stock material.

$$E_d = \frac{P}{v \cdot d} \qquad (1)$$

As the energy density is governed by the scan speed, v, spotsize, d, and laser power, P, it is necessary to be able to control or quantify the mentioned parameters. The homogeneity of the weld bead is influenced by several constituents, therefore, any inhomogeneity found in the welded track must be considered a combination of any number of irregularities.

Consideration of the process parameters allows optimization of the process. However, to get a thorough understanding of the system, machine parameters should be characterised with the same care as process parameters and the parts produced.

This work proposes a method to identify and quantify the effect of the thermal lensing, induced by thermal distortion of the optical elements.

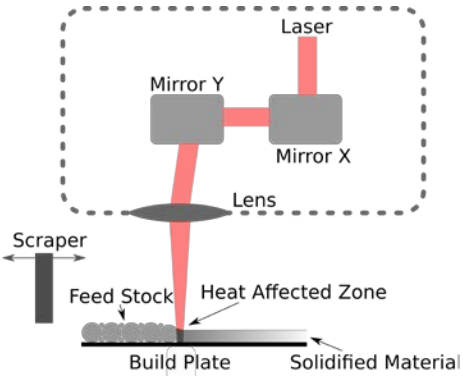

Figure 1. Principal sketch of the experimental setup used.

2. Method

To identify the cause and effect of the weld track widening a method applying different approaches was implemented. Initially the identification of the irregularity was carried out by performing weld tracks, and evaluating the tendencies of the discrepancy. Next, the cause was located by isolating and quantifying the scan velocity and power absorption along the beam path. Finally, the condition of the optical element was visually inspected.

The current setup include; a custom single layer experimental powder handling unit, an fθ scan lens (Thorlabs FTH254-1064), a galvanometer (Thorlabs GVS012) as scan head with silver coated mirrors, and, a 250W continuous wave fiber laser (SPI SP-250C-W-HS-S-06-QCS) with a wavelength of 1070nm, see figure 1.

2.1. Weld Tracks

To investigate the influence of different parameters, a range of experiments was carried out altering the direction, power and speed of the laser beam trajectory. The feed stock material used in these experiment was 316L stainless steel powder.

Experiments were carried out to clarify the circumstances in which the weld track became unstable, see figure 2. Single line melt tracks (16 mm) were made to measure the changes in quality when the duration of emission was increased. These were altered between running with a continuous laser emission, and running a single line and then implementing a break identical to the scan time, thus allowing the system to cool down in between scans. Squares with overlapping tracks (16 mm x 16 mm) were likewise scanned. Finally, one long rectangular scan track (244 mm) was carried out to observe the extent of the irregular melt pool.

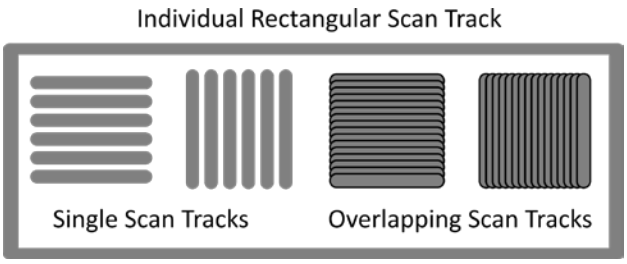

Figure 2. Scans performed in 316L stainless steel powder. All scans was performed with a parallel scanning strategy.

2.2. Scan Velocity

To ensure the widening of the weld track is not caused by a change in speed the scan velocity of the laser beam was measured using a photo detector (Thorlabs DET10A), see figure 3. The duration of the laser emission was accurately measured while scanning single lines at varying scan velocities. To obtain the scanning velocity, the duration of the emission was coupled with the measured track length.

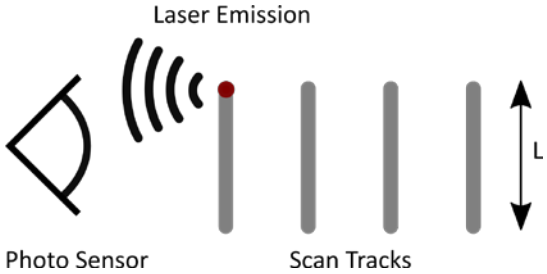

Figure 3. Principal sketch of a method for obtaining the scan velocity by detecting the duration of each scan track and measuring the length of the track.

2.3. Power Detection

To obtain a relative relation between the power transmitted (50 W - 110 W) throughout the system, a power detector (Gentec-eo UP55M-500W-H12) was installed at various stages in the setup, see figure 4. Initially, the power was measured before the scan head and scan lens to obtain baseline measurements. Next, the power reading was taken after the beam was reflected on the mirrors mounted on the galvanometers in the scan head. The final reading was performed with all the optical components in place, including both the scan head and the scan lens. Each measurement was taken as an average over 10 s and, repeated 3 times. The data was then used to extrapolate the trends to the full range of laser powers.

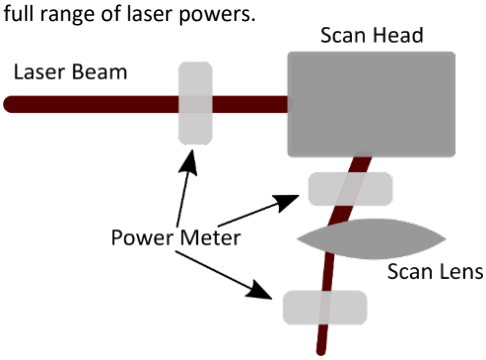

Figure 4. Principal sketch of power detector measurements made in between each optical element.

2.4. Visual Inspection

To allow a visual inspection of the state of the mirror, an experimental setup was created including only one mirror as the optical component, see figure 5. The reflected beam was disposed into a water-cooled aluminium block, used as beam dump. Two mirrors were tested with this setup, initially a silver-coated mirror identical to the one used in the original setup, and in addition another mirror with a dielectric coating. Both the silver-coated and dielectric mirror were rated to be able to withstand the 250 W, at 1070 nm.

The laser was emitting for different periods of time (10 s to 40 min) and at varying power levels (25 W to 250 W with intervals of 25 W).

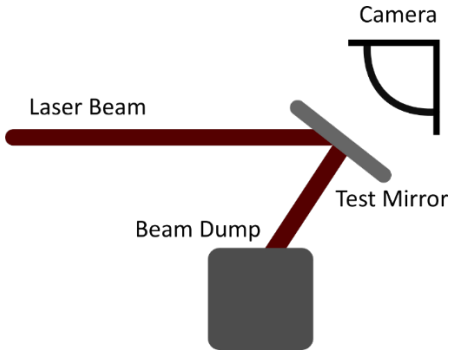

Figure 5. Principal sketch of the experimental setup used to visually inspect the behaviour of mirrors exposed to laser emission.

3. Results

Upon conducting single layer experiments with the open architecture system, it became obvious that the weld tracks showed inhomogeneous behaviour. To identify and quantify the source of this error a characterisation of the system was carried out.

3.1. Identification of irregularities

Experiments showed that the scan tracks became irregular and widened as the duration of the scan increased. Running individual 16 mm scan tracks, with constant beam emission, displays that the instability increased in each consequent weld track. Demonstrated in figure 6, the melt pool characteristics changes as scan lines L1, L2 and L3 is made. The melt pool becomes wider and the depth of penetration lower as more scan tracks are made at the same process parameter. This experiment was done varying the direction, speed and laser power, consistently displaying a decrease in stability as the duration of laser emission increased.

Hereafter overlapping tracks in the form of squares was made, introducing a pause between each scan line, allowed the system to stabilise and cool down between scans. Hence, the weld tracks was observed homogeneous at the beginning of consequent scans, see figure 7 (a). However by the end of each track, figure 7 (b), the melt pool became unstable, and balling became the predominant outcome.

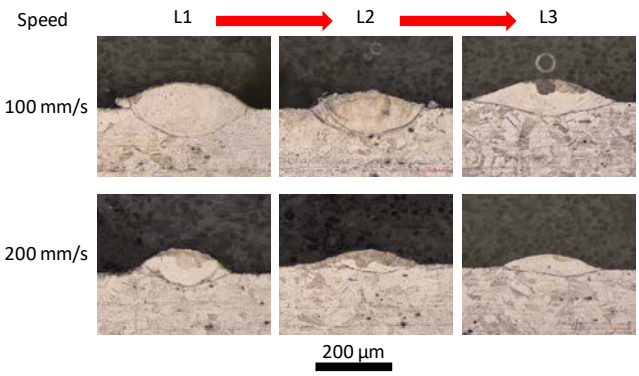

Figure 6. Single line weld tracks, conducted (L1 -> L2 -> L3) without any pause between lines. The melt pool depth decreases as the exposure duration rises.

Scan Direction

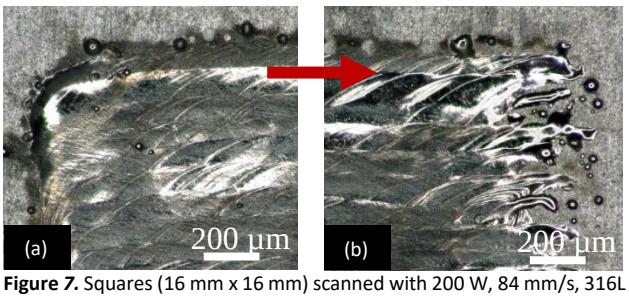

Figure 7. Squares (16 mm x 16 mm) scanned with 200 W, 84 mm/s, 316L stainless steel powder. At the beginning of each line in the melted track (a) the melt pool is uniform. At the end of each scan line the melt pool behaves irregular (b).

To observe if this tendency got worse as the scan track was prolonged, one 244 mm scan track was performed. The beginning of the track demonstrates homogeneous behaviour, figure 8(a), thereafter the melt pool widens midway to 130 %, from initial 255 µm to 330 µm, figure 8(b). Finally, after 183 mm the melt pool became unstable to an extent where the melt pool consist predominantly of balling, figure 8(c). In figure 9 the melt pool width was observed to consistently increase along the track, showing an increase in variation as the trajectory changes direction at the corners of the rectangular single line weld track.

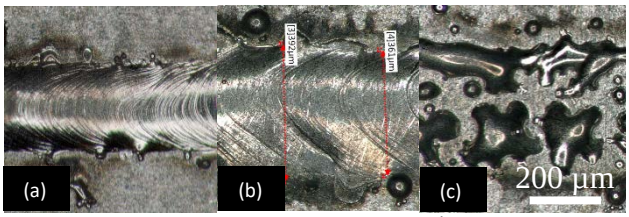

Figure 8. Scanned track of 244 mm, 200 W, 84 mm/s, 316L stainless steel powder. At the beginning of the melted track (a) the melt pool width is most narrow. Along the track (b) the width increases, until it finally fails (c).

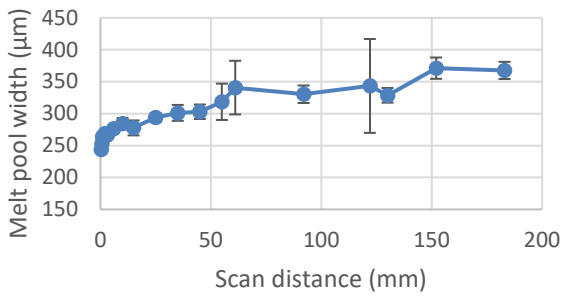

Figure 9. Representation of the widening of the melt pool as the scan distance increases

3.2. Stability of scan velocity

Detection of when the beam starts and stops during single track scan was achieved by recording the light emission from the weld track using a photodiode, see figure 10.

Due to the open architecture construction of hardware, electronics and software, the scan velocity was matched against a machine parameter, the F-number which determines the scan velocity. In figure 11, a linear relationship between the scan velocity and varying F-number settings can be seen. Each measurement was repeated 4 times and the error was always observed to be lower than 1 %. Thus the scan velocity was well calibrated.

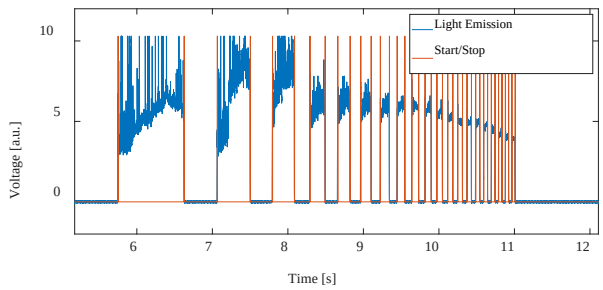

Figure *10.* Recording of light emitted from processing of individual scan tracks, marking the start and stop time for each track.

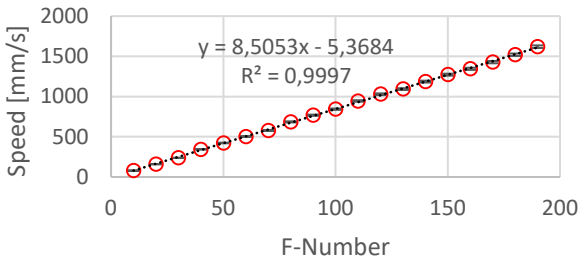

Figure *11.* Linear approximation of the relation between scan velocity and different machine (F) values determining the velocity. Less than 1 % error on each data point.

3.3. Power absorbed in optical elements

The raw beam measured by the power detector showed a linear trend, but 15 % higher than the internal power controller of the laser. Measuring the power present after the scan head showed a substantial power decrease. Last measurement was after both the scan head and the scan lens, here the difference was [redacted] nguishable from the previous, see figure 12.

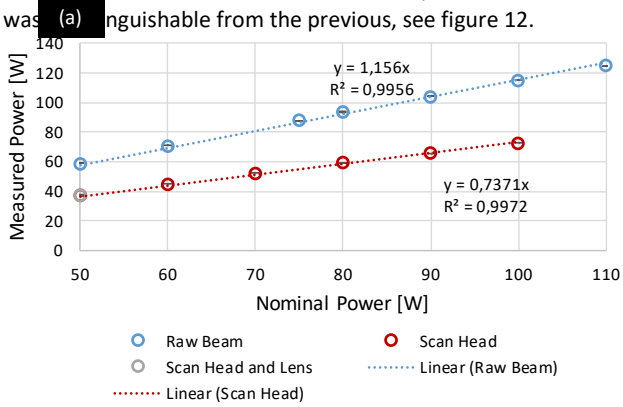

Figure 12. Power measured between the optical elements.

As the initial measurement showed the raw beam power to be exceeding the nominal power, the relative loss between the measured raw beam and the scan head was calculated using the linear approximation previously presented in figure 12. Figure 13 demonstrates an expected 42 % power absorption by the mirrors in the scan head, across the operational range of the laser.

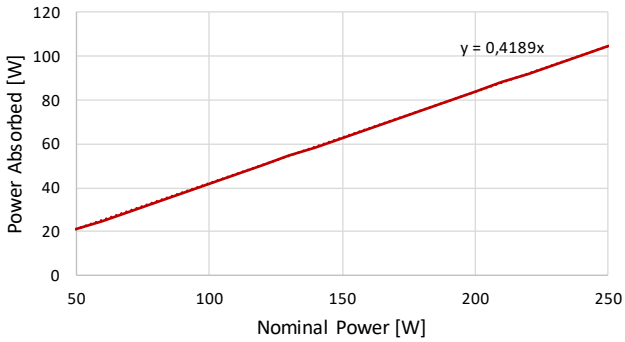

Figure 13. Power absorbed by the silver-coated mirrors in the scan head.

3.4. Degenerating mirrors

Having determined that the mirrors in the scan head were responsible for the dominant power loss, these were inspected visually during laser emission. Two different coatings were tested, one silver coated and another dielectrically coated.

The silver coated mirror was exposed for 10 s with the power level ranging from 25 W to 125 W, before a visual mark was left on the coating, see figure 14(a). Similar experiments were carried out with a dielectric coated mirror. Opposed to the silver coated mirror, the dielectric coated mirror was able to withstand 250 W with an exposure time of 40 min (2400 s) without any visual damage, see figure 14(b).

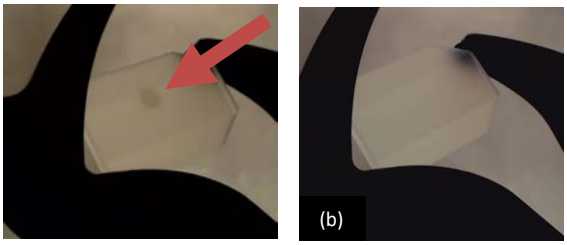

Figure 14. Visual inspection of the differently coated mirrors. (a) silver-coated mirror, the burn mark on the mirror becomes visible at 125 W at a 10 s exposure time. (b) dielectric coated mirror, the mirror stays visually intact exposing it to 250 W for 40 min.

4. Summary

It was demonstrated that the scan velocity was consistent across different speeds and positions. Furthermore, the melt pool was observed to widen significantly along a 244 mm scan track to 130 % of the initial width, hereafter it becomes so wide that the melt pool was unable to penetrate the substrate and balling became predominant.

The widening of the melt pool was investigated by considering thermal distortion of the mirrors. To achieve an idea of how much power was lost to each optical element a power detector was used to demonstrate that the silver-coated scan mirrors consumed 42 % of the initial beam power. Therefore thermal lensing of the silver-coated mirrors was suspected to influence the inhomogeneous melt pool observed.

Visual inspection of the silver-coated mirrors showed that the coating started to deteriorate at 125 W with an exposure time of 10 s. Deeming it unfit for L-PBF with a laser beam of 1070nm and 125W, a replacement mirror with a dielectric coating was tested, proving to not visually alter at 250 W with an exposure time of 40 min (2400 s).

5. Conclusion

This paper has presented a method for identifying thermal lensing as one of the sources of irregular weld tracks by initially isolating possible error sources, and then quantifying the extent of the power lost to optical component. Thus including thermal

distortions and degeneration of the optical elements as a significant constituent causing inhomogeneous weld tracks.

The method served as an effective mean for isolating the cause of thermal lensing based upon identification of effect (weld widening) and a systematic mapping of loss throughout the beam path. This method also allows for quantification of the power lost throughout the beam path.

The results determines that a silver-coated mirror, rated to withstand the power and laser used, turned out to degenerate as heat dissipated into the mirror. Causing thermal lensing until the point of failure. Replacing the silver-coated mirror has shown promising results, as the visible damage and failure was avoided even at high power and long exposure times.

Within this work it became clear that the vast number of parameters influencing the quality of the parts produced with L-PBF has to include identification and quantification of the thermal influence and possible instability of the optical elements.

References

[1] ASTM International, "BS ISO/ASTM 52900:2015 Additive manufacturing. General principles. Terminology," *Rapid Manufacturing Association*. pp. 10–12, 2013.

[2] C. Thiel, ; Stubenvoll, ; Schäfer, and ; Krol, "Reliable Beam Positioning for Metal-based Additive Manufacturing by Means of Focal Shift Reduction," 2015.

[3] L. R. Goossens, Y. Kinds, J.-P. Kruth, and B. Van Hooreweder, "on the Influence of Thermal Lensing During Selective Laser," *Solid Free. Fabr. Symp. – An Addit. Manuf. Conf.*, no. Solid Freeform Fabrication 2018: Proceedings of the 29th Annual International, pp. 2267–2274, 2018.

[4] Z. Y. Y. Liu, C. Li, X. Y. Y. Fang, and Y. B. B. Guo, "Energy Consumption in Additive Manufacturing of Metal Parts," *Procedia Manuf.*, vol. 26, pp. 834–845, 2018.